

Towards Better Evaluation of GNN Expressiveness with BREC Dataset

Yanbo Wang Muhan Zhang*
 Institute for Artificial Intelligence, Peking University
 yanxwb202@gmail.com, muhan@pku.edu.cn

Abstract

Research on the theoretical expressiveness of Graph Neural Networks (GNNs) has developed rapidly, and many methods have been proposed to enhance the expressiveness. However, most methods do not have a uniform expressiveness measure except for a few that strictly follow the k -dimensional Weisfeiler-Lehman (k -WL) test hierarchy. Their theoretical analyses are often limited to distinguishing certain families of non-isomorphic graphs, leading to difficulties in quantitatively comparing their expressiveness. In contrast to theoretical analysis, another way to measure expressiveness is by evaluating model performance on certain datasets containing 1-WL-indistinguishable graphs. Previous datasets specifically designed for this purpose, however, face problems with difficulty (any model surpassing 1-WL has nearly 100% accuracy), granularity (models tend to be either 100% correct or near random guess), and scale (only a few essentially different graphs in each dataset). To address these limitations, we propose a new expressiveness dataset, **BREC**, which includes 400 pairs of non-isomorphic graphs carefully selected from four primary categories (Basic, Regular, Extension, and CFI). These graphs have higher difficulty (up to 4-WL), finer granularity (able to compare models between 1-WL and 3-WL), and a larger scale (400 pairs). Further, we synthetically test 16 models with higher-than-1-WL expressiveness on our BREC dataset. Our experiment gives the first thorough comparison of the expressiveness of those state-of-the-art beyond-1-WL GNN models. We expect this dataset to serve as a benchmark for testing the expressiveness of future GNNs. Our dataset and evaluation code are released at: <https://github.com/GraphPKU/BREC>.

1 Introduction

GNNs are graph-based machine learning models that have been widely used in bioinformatics, recommender systems, social network analysis, and other fields with excellent results [Duvenaud et al., 2015, Barabási et al., 2011, Fan et al., 2019, Wang et al., 2018a, Berg et al., 2017, Zhou et al., 2020]. Although achieving great empirical successes in various fields, related studies have shown that GNNs have limited ability to distinguish non-isomorphic graphs, such as regular graphs of the same size and degree. Xu et al. [2018] established a connection between the expressiveness of message passing neural networks (MPNNs) and the WL algorithm for graph isomorphism testing, showing MPNN’s upper bound is 1-WL. Many subsequent studies have proposed GNN variants with improved expressive power [Balcilar et al., 2021, Bevilacqua et al., 2021, Cotta et al., 2021, Morris et al., 2019, You et al., 2021, Zhang and Li, 2021].

With so many models based on different schemes (such as injecting features, following WL hierarchy, maintaining equivariance, and extracting subgraphs), it is greatly desired to have a unified framework that can theoretically compare the expressive power between different variants. Maron et al. [2018]

* Corresponding author.

propose the k -order invariant/equivariant graph networks which unify linear layers keeping permutation invariance/equivariance. Frasca et al. [2022] unifies recent subgraph GNNs and proves their expressiveness upper bound is 3-WL, while Zhang et al. [2023a] builds a complete expressiveness hierarchy of subgraph GNNs by giving counterexamples between each pair. However, it is still unknown how large the gaps are. Moreover, there exist methods hardly categorized by the k -WL hierarchy. For example, Papp and Wattenhofer [2022] proposes four extensions of GNNs, each of which cannot strictly compare with the other. Feng et al. [2022] propose a GNN that is partly stronger than 3-WL, yet at the same time cannot distinguish many 3-WL-distinguishable graphs. Huang et al. [2022] propose to evaluate expressiveness through counting certain important substructures (such as 6-cycles). Zhang et al. [2023b] introduce graph biconnectivity to test expressiveness.

When a unified theoretical characterization of expressiveness does not exist, testing on expressiveness datasets is a good approach. Abboud et al. [2020], Murphy et al. [2019], Balcilar et al. [2021] propose three expressiveness datasets EXP, CSL, and SR25, which have been widely used in recent studies on powerful GNNs. However, these datasets have significant limitations. First, the datasets do not have sufficient difficulty. The EXP and CSL datasets include only 1-WL failure examples, and most GNN variants in recent years can achieve 100% accuracy. Second, the granularity of the datasets is too coarse. That is, these datasets include only graphs generated by one method with the same discrimination difficulty. Thus, the performance of GNN variants is often either 0 (completely indistinguishable) or 100% (completely distinguishable), making it difficult to provide a fine-grained expressiveness measure or comparison. Finally, the size of the datasets is too small, containing only a few to a few dozen substantially different graphs, and may not be generalizable.

To address the limitations of existing expressiveness datasets, we propose a new dataset, BREC, which includes 400 pairs of non-isomorphic graphs in 4 major categories, namely Basic graphs, Regular graphs, Extension graphs, and CFI graphs, whose difficulty ranges from 1-WL to 4-WL. Compared to existing datasets, BREC has a greater difficulty (up to 4-WL), finer granularity (able to compare models between 1-WL and 3-WL), and larger scale (400 pairs of graphs each of which is essentially different from others), addressing the shortcomings of previous datasets.

Due to the increased size and diversity of the dataset, the traditional classification task may not be suitable for training-based evaluation methods which rely on generalization ability. Thus, we propose a new principled evaluation procedure based on directly comparing the differences between model outputs. Considering the influence of numerical precision, we propose reliable paired comparisons improved from a statistical method [Johnson and Wichern, 2007], with a precise bound of errors. Experiments verify that this new evaluation procedure aligns well with known theoretical results.

Finally, we compare 16 representative beyond-1-WL models on BREC. Our experiments, for the first time, give a **reliable empirical comparison** of state-of-the-art GNNs' expressiveness. The currently most thorough expressiveness comparison can serve as a good start to more deeply understanding different schemes for improving GNNs' expressive power. On BREC, GNN accuracies range from 41.5% to 70.8%, with I²GNN [Huang et al., 2022] performing the best. The 70.8% highest accuracy also implies that the dataset is **far from saturation**. We expect BREC can serve as a benchmark for testing future GNNs' expressiveness. We also welcome contributions and suggestions to improve BREC. Our dataset and evaluation code are included in <https://github.com/GraphPKU/BREC>.

2 Limitations of Existing Datasets

Preliminary. We use $\{ \}$ to denote sets and use $\{ \{ \}$ to denote multisets. The cardinality of (multi)set \mathbb{S} is denoted as $|\mathbb{S}|$. The index set is denoted by $[n] = \{1, \dots, n\}$. Denote a graph as $\mathcal{G} = (\mathbb{V}(\mathcal{G}), \mathbb{E}(\mathcal{G}))$ with sets of *nodes* or *vertices* $\mathbb{V}(\mathcal{G})$ and *edges* $\mathbb{E}(\mathcal{G})$. Without loss of generality, we set $|\mathbb{V}(\mathcal{G})| = n$ and $\mathbb{V}(\mathcal{G}) = [n]$. A graph is called undirected if $(u, v) \in \mathbb{E}$ iff. $(v, u) \in \mathbb{E}$. The permutation (or reindexing) of \mathcal{G} is denoted as $\mathcal{G}^\pi = (\mathbb{V}(\mathcal{G}^\pi), \mathbb{E}(\mathcal{G}^\pi))$ with permutation $\pi : [n] \rightarrow [n]$, s.t. $(u, v) \in \mathbb{E}(\mathcal{G}) \iff (\pi(u), \pi(v)) \in \mathbb{E}(\mathcal{G}^\pi)$. We do not include node or edge features in definitions to simplify the description. Further discussions of them can be found in Appendix B.

Graph Isomorphism (GI) Problem. We say that two graphs \mathcal{G} and \mathcal{H} are isomorphic (denoted $\mathcal{G} \simeq \mathcal{H}$) if there exists a bijection $\phi : \mathbb{V}(\mathcal{G}) \rightarrow \mathbb{V}(\mathcal{H})$, s.t. $(u, v) \in \mathbb{E}(\mathcal{G})$ iff. $(\phi(u), \phi(v)) \in \mathbb{E}(\mathcal{H})$. GI is essential for studying GNN's expressiveness. Supposing two non-isomorphic graphs \mathcal{G} and \mathcal{H} , only if a GNN model f successfully distinguishes them, i.e., $f(\mathcal{G}) \neq f(\mathcal{H})$, can they be further assigned different labels. Some researchers [Chen et al., 2019, Geerts and Reutter, 2022] point out

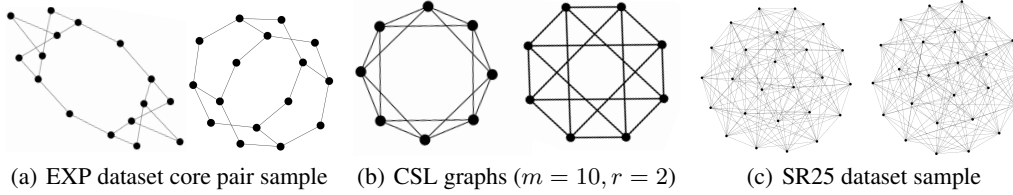


Figure 1: Sample graphs in previous three datasets

Table 1: Dataset statistics

Dataset	# Graphs	# Core graphs	# Nodes	Hardness	Metrics
EXP	1200	6	33-73	1-WL	2-way classification
CSL	150	10	41	1-WL	10-way classification
SR25	15	15	25	3-WL	15-way classification
BREC	800	800	10-198	1-WL to 4-WL	Reliable Paired Comparisons

the equivalence between GI and function approximation, showing the importance of GI. However, GI is suspected to be NP-hard. A naive solution has to iterate all $n!$ permutations to test the bijection.

Weisfeiler-Lehman algorithm (WL). WL is a classical isomorphism test based on color refinement [Weisfeiler and Leman, 1968]. Each node keeps a state (or color) that gets refined in each iteration by aggregating information from its neighbors’ states. The final graph representation is a multiset of node states after convergence. Though WL can identify most non-isomorphic graphs, it may fail in some simple graphs, which motivates some extended versions. For example, k -WL treats each k -tuple of nodes as a unit for aggregating information. Another slightly different method [Cai et al., 1989] is also called k -WL sometimes. We follow Morris et al. [2019] to call the former one k -WL, while the latter one k -FWL. More details can be found in Appendix C.

Considering the importance of GI and WL, some relevant expressiveness datasets based on them are proposed, and the three most commonly used datasets are as follows. We sample a pair of graphs from each to visualize in Fig 1. Their statistics are shown in Table 1.

EXP Dataset. This dataset consists of 600 pairs of non-isomorphic graphs which 1-WL fails. The generation process for each pair is as follows. Each graph of the pair includes two disconnected components. The first component is called the core pair, and that part of the two graphs is non-isomorphic, satisfying different SAT conditions. The second component is called the planar component, which is identical in the two graphs. The planar component is primarily introduced to create noise in the dataset and make learning more challenging. Only the core pair can test expressiveness. However, this component is produced in relatively small quantities. Only **three substantially different**, 1-WL-indistinguishable core pairs exist in the dataset.

This dataset labels each graph by whether its core component satisfies a particular SAT problem, and then requires training a binary classification model. Although this dataset solves the problem of semantic labeling by introducing the SAT problem and extends the size and richness by including planar components, due to the simplicity of the core pair generation and the insufficient number, most recent GNNs easily achieve nearly 100% accuracy, making it difficult to compare their expressiveness.

CSL Dataset. This dataset consists of 150 Circulant Skip Links (CSL) graphs, on which 1-WL test fails. The CSL graph is defined as follows. Let r and m be co-prime natural numbers such that $r < m - 1$. $\mathcal{G}(m, r) = (\mathbb{V}, \mathbb{E})$ denotes an undirected 4-regular graph with $\mathbb{V} = [m]$ whose edges form a cycle and have skip links. That is, for the cycle, $(j, j + 1) \in \mathbb{E}$ for $j \in [m - 1]$ and $(m, 1) \in \mathbb{E}$. For the skip links, recursively define the sequence $s_1 = 1, s_{i+1} = (s_i + r) \bmod m + 1$ and let $(s_i, s_{i+1}) \in \mathbb{E}$ for any $i \in \mathbb{N}$. Setting $m = 41, r = \{2, 3, 4, 5, 6, 9, 11, 12, 13, 16\}$, we obtain 10 CSL graphs that are distinct from each other. Further, 14 corresponding graphs are generated for each distinct CSL graph by random node reindexing. Thus the final dataset contains 150 graphs.

This dataset treats each of the 10 CSL graphs as a separate class and requires training a 10-way classification model. Although it provides a way to generate 4-regular graphs with any number of nodes, the final dataset consists of only **ten essentially different** regular graphs with the **same number of nodes and degree**. Since a majority of recent expressive GNNs handle regular graphs well (especially with a fixed number of nodes and degree), most can achieve close to 100% accuracy.

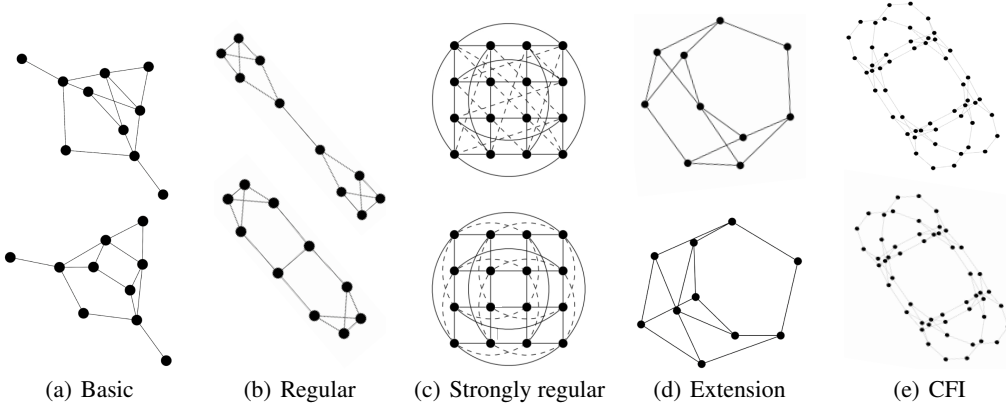


Figure 2: BREC dataset samples

SR25 Dataset. This dataset consists of 15 strongly regular graphs, on which the 3-WL test fails. Each graph is a strongly regular graph with 25 nodes and a degree of 12. The connected nodes share 5 common neighbors, and the non-connected nodes share 6. In actual use, SR25 is translated to a 15-way classification problem with the goal of mapping each graph into a different class, where the training and test graphs overlap.

Nowadays, 3-WL is the upper bound for most of the proposed expressive GNNs. Thus a wide range of methods only obtain 6.67% (1/15) accuracy in SR25. Moreover, since all strongly regular graphs in SR25 have the same parameters, existing methods tend to have either **completely indistinguishable** (6.67%) or **completely distinguishable** (100%) performance [Feng et al., 2022], making it difficult to give a fine-grained expressiveness measure.

Summary. These three datasets have limitations regarding difficulty, granularity, and scale. In terms of difficulty, these datasets are all bounded by 3-WL, failing to evaluate models (partly) beyond 3-WL [Feng et al., 2022, Huang et al., 2022]. In terms of granularity, the graphs are generated in one way, and the parameters of the graphs are repetitive, which easily leads to 0/1 step function of model performance and cannot measure subtle differences between models. In terms of scale, the number of substantially different graphs in the datasets is small, and the test results may not be generalizable.

3 BREC: A New Dataset for Expressiveness

In this section, we propose a new expressiveness dataset called BREC, which consists of four major categories of graphs: Basic, Regular, Extension, and CFI. Basic graphs consist of relatively simple 1-WL-indistinguishable graphs. Regular graphs include a variety of subcategorized regular graphs, such as simple regular graphs and strongly regular graphs, which can guide related research. Extension graphs mainly contain special graphs found when comparing four kinds of GNN extensions [Papp and Wattenhofer, 2022], which can better characterize the gap between 1-WL and 3-WL. CFI graphs mainly include graphs generated by the CFI methods [Cai et al., 1989], which have greater difficulty and larger graph sizes. With the combination of the above four classes of graphs, our BREC dataset addresses previous datasets’ limitations in difficulty, granularity, and scale. We show samples from the four categories in Fig 2.

3.1 Dataset Composition

BREC includes 400 pairs of non-isomorphic graphs, with detailed composition as follows:

Basic Graphs. Basic graphs consist of 60 pairs of 10-node graphs collected from an exhaustive search. These graphs are not regular graphs and are indistinguishable by 1-WL, but most can be distinguished by expressive GNN variants. This part is the simplest part and sanity check in BREC.

Basic graphs can also be considered as an enhancement of the EXP dataset as they both use non-regular 1-WL-indistinguishable graphs. However, Basic graphs provide more examples and richer graph patterns than EXP. The relatively small graphs also facilitate visualization and analysis.

Regular Graphs. This part consists of 140 pairs of regular graphs, including 50 pairs of simple regular graphs, 50 pairs of strongly regular graphs, 20 pairs of 4-vertex condition graphs, and 20 pairs of distance regular graphs. Each pair of graphs possess the same parameters. A graph in which all nodes have the same degree is a regular graph. Regular graphs cannot be distinguished by 1-WL, and some studies analyze GNN expressiveness from this aspect [Li et al., 2020, Zhang and Li, 2021]. We denote regular graphs that do not possess special properties as simple regular graphs. When considering more difficult regular graphs, strongly regular graphs (3-WL fails) are often introduced. Strongly regular graphs further require that the number of neighboring nodes of any two nodes depends only on whether the two nodes are connected. A pair of common examples are 4×4 -Rook’s graph and Shrikhande graph (shown in Fig 2(c)). Among them, the 4×4 -Rook’s graph also satisfies the 4-vertex condition property [Brouwer et al., 2021], where the number of connected edges between the common neighbors of any two nodes depends only on whether these two nodes are connected. The diameter of a connected strongly regular graph is always 2 [Brouwer et al., 2012a]. So in order to extend the graph’s diameter, there exists an even more difficult graph called the distance regular graph [Brouwer et al., 2012b]. A distance regular graph is a regular graph such that for any two vertices v and w , the number of vertices at a distance j from v and at a distance k from w depends only upon j, k and the distance between v and w . Strongly regular graphs are, in fact, a particular case of distance regular graphs with a diameter of 2. For a more detailed discussion of their relationship, please refer to Appendix A

This part can be regarded as an enhancement to the CSL and SR25 datasets. It includes more subdivisions of regular graphs, including simple regular graphs, strongly regular graphs, 4-vertex condition graphs, and distance regular graphs, providing a wider difficulty range and a higher difficulty upper bound. Furthermore, it does not restrict all regular graphs in a category to share the same parameters, thus greatly enhancing the diversity.

Extension Graphs. This part consists of 100 pairs of extension graphs inspired by Papp and Wattenhofer [2022]. This paper proposed four types of theoretical GNN extensions: k -WL hierarchy-based, substructure-counting-based, k -hop-subgraph-based, and marking-based methods, and compared their expressiveness theoretically (which indicates most of them are not comparable). We generated 100 pairs of graphs based on the counterexamples in their theoretical analysis as well as some actual searched results. All the 100 pairs of graphs can be distinguished by 3-WL but not by 1-WL.

The graphs in this part were not considered in the previous datasets. They mainly serve the purpose of improving the dataset’s granularity between 1-WL and 3-WL.

CFI Graphs. This part consists of 100 pairs of CFI graphs based on Cai et al. [1989]. They developed a method to generate graphs distinguishable by k -WL but not by $(k - 1)$ -WL. We generated 100 pairs of graphs based on this method up to 4-WL-indistinguishable, which is far more than enough for current research. In particular, 60 pairs are only 3-WL-distinguishable, 20 pairs are only 4-WL-distinguishable, and 20 pairs are even 4-WL-indistinguishable.

This part of the dataset was also not considered in the previous datasets. As the most challenging part of BREC, CFI graphs further raise the upper limit of difficulty. The graph size of this part is also larger than the other parts (up to 198 nodes), which makes the dataset more challenging by placing a higher demand on the model’s ability to process graphs with heterogeneous sizes.

3.2 Advantages

We summarize how BREC addresses the three problems.

Difficulty. BREC provides more difficult graphs than previous ones. The CFI method can generate a graph distinguishable by $(k + 1)$ -WL but not by k -WL. We provide graphs with a maximum difficulty of 4-WL following it. We also include 4-vertex condition graphs and distance regular graphs, which are variants of strongly regular graphs (3-WL-indistinguishable) with greater difficulty.

Granularity. The various difficulty levels of the different classes of graphs are as follows. Basic graphs contain some basic 1-WL-indistinguishable graphs, which serve a similar role to the EXP dataset. The major components of regular graphs are simple regular graphs and strongly regular graphs, on which 1-WL and 3-WL fail, respectively. They can be considered an extension of the CSL dataset and SR25 dataset. Regular graphs also contain 4-vertex condition and distance regular graphs, which further raise the difficulty level. Extension graphs contain graphs whose difficulty span

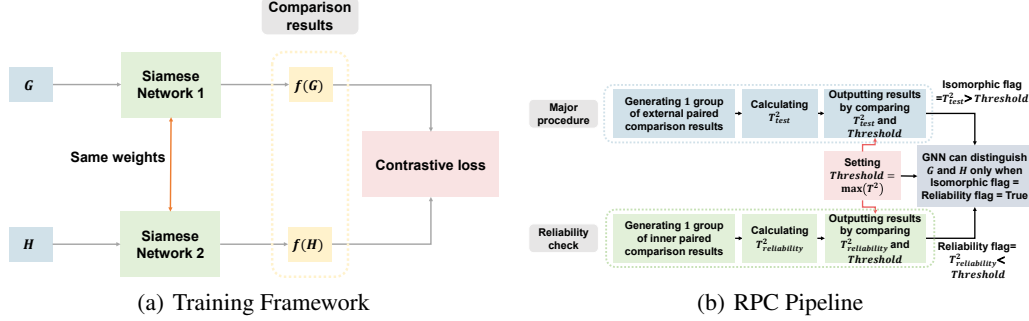


Figure 3: Evaluation Method

between 1-WL and 3-WL, which can be used to compare many beyond-1-WL models in a more fine-grained way. CFI graphs contain graphs ranging from 1-WL to 4-WL difficulty.

Scale. As we mentioned before, the previous datasets used only tens of essentially different graphs to generate the dataset. Our dataset uses 800 essentially different graphs, greatly expanding the diversity and scale. In particular, since the previous datasets used a small number of graphs, relevant statistics such as the distribution of graph sizes, degrees and diameters are also restricted. For example, the number of nodes and diameters are the same for all graphs in CSL and SR25. In contrast, our dataset has a much richer distribution. Related statistics are displayed in Appendix D

4 RPC: A New Evaluation Method

In this section, we propose a training framework and an evaluation method for BREC. Previous datasets all adopt a classification setting, i.e., give each graph a label, train a classification model, and evaluate the accuracy on test graphs as the expressiveness measure. There are two ways to give labels in the previous datasets: the EXP dataset provides a semantic label based on whether the core component satisfies the SAT condition, and the CSL and SR25 datasets give a distinct label for each essentially different graph. However, neither of these two labeling schemes is applicable to BREC. First, to enrich the data generation methods and the diversity of graphs, BREC does not associate a semantic label to each graph like using a particular SAT problem (which significantly restricts the space of possible graphs). Second, simply giving each graph a distinct label would transform BREC into an 800-class classification problem whose performance is greatly affected by factors other than expressiveness (such as the difficulty of training). Therefore, our core idea instead is to measure the “separating power” of a model directly. This is also why BREC is organized pair-wise. Each pair is tested individually to return whether a GNN can distinguish them.

However, how can we say a pair of graphs is successfully distinguished? Previous researchers tend to set a small threshold (like $1E-4$) manually. If the embedding distance between two graphs is larger than the threshold, the GNN is considered to distinguish them. This method lacks **reliability** due to numerical precision, especially facing graphs varying in size. In order to produce reliable results, we propose an evaluation method measuring both **external difference** and **internal fluctuations**. We also propose a training framework for pair-wise data points with siamese network design [Koch et al., 2015] and contrastive loss [Hadsell et al., 2006, Wang et al., 2018b], which enlarges the distance between their output embeddings. The pipeline is shown in Fig 3(a).

4.1 Training Framework

We follow the siamese network design approach [Koch et al., 2015] to train the model for each pair of graphs to distinguish. The main body of the network is the two identical models that always keep the same parameters. Inputting a pair of graphs generates a pair of embeddings. Then the distance between them is measured by cosine similarity. The loss function is as follows:

$$L(f, \mathcal{G}, \mathcal{H}) = \text{Max}(0, \frac{f(\mathcal{G}) \cdot f(\mathcal{H})}{\|f(\mathcal{G})\| \|f(\mathcal{H})\|} - \gamma), \quad (1)$$

where the GNN model $f : \{\mathcal{G}\} \rightarrow \mathbb{R}^d$, \mathcal{G} and \mathcal{H} are two non-isomorphic graphs, and γ is a margin hyperparameter (set to 0 in our experiments). The loss encourages the cosine similarity to be less than γ , pushing two graph embeddings away from each other.

The training process can **benefit models** in multiple aspects. Firstly, it can help GNN reach its theoretical expressiveness. In the theoretical analysis of GNN expressiveness, only the structure of the network is generally considered without restricting the parameters of the network, which means we are actually exploring the expressiveness of **one group of functions**. If one model with specific parameters can distinguish a pair, then the model design and structure are considered expressive enough to distinguish them. However, we cannot iterate all possible parameter combinations to test the real upper bound, which is why we choose training. Training can **realize searching** in the function space, leading to a better practical expressiveness. In addition, training can help model components reach specific properties such as injective and universal approximation, which are crucial for reaching the theoretical power. These properties require specific parameters to be achieved, and a network with randomly initialized parameters may not satisfy these properties. Moreover, training can make model-distinguishable graph pairs **more easily discriminated** from model-indistinguishable pairs, and reduce false negative rate caused by numerical precision. This is because, by pair-wise contrastive training, the distance between two graphs' embeddings will be further enlarged if they are distinguished by the model, but will not change much when the two graphs are not distinguished and their distance is only numerical error. The training framework is shown in Fig 3(a).

4.2 Evaluation Method

Recall that we choose to directly compare the output of GNNs on a pair of non-isomorphic graphs to measure expressiveness. If there is a significant difference, then the GNN is considered to be able to distinguish them. However, how to set the threshold is a problem. A large threshold may produce many false negatives (the model is expressive enough to distinguish them but the difference is less than the threshold), while a small threshold may produce many false positives (the model cannot distinguish them but the fluctuating/numerical errors make the difference larger than the threshold).

Paired Comparisons [Johnson and Wichern, 2007] is a classical method for comparing two groups of results with fluctuating errors. Instead of comparing a single pair of results, it repeatedly generates results for each target and compares two groups of results to reduce the influence of random errors. We improve upon this method to check whether a GNN really outputs different results for a pair of graphs, named **Reliable Pairwise Comparison (RPC)**. The pipeline is shown in Fig 3(b).

RPC has two components: Major procedure and Reliability check. The Major procedure is conducted on a pair of non-isomorphic graphs to capture their difference, while the Reliability check is conducted on graph automorphisms to capture internal fluctuations caused by numerical precision.

Major procedure. Given a pair of non-isomorphic graphs \mathcal{G}, \mathcal{H} , we generate q copies for each by random reindexing to form two groups of graphs. Each copy is represented as:

$$\mathcal{G}_i, \mathcal{H}_i, i \in [q]. \quad (2)$$

We utilize Paired Comparisons on the two groups. Supposing the GNN function is $f : \{\mathcal{G}\} \rightarrow \mathbb{R}^d$, we first calculate q differences:

$$\mathbf{d}_i = f(\mathcal{G}_i) - f(\mathcal{H}_i), i \in [q]. \quad (3)$$

Assumption 4.1. \mathbf{d}_i are independent $\mathcal{N}(\boldsymbol{\mu}, \boldsymbol{\Sigma})$ random vectors.

The above assumption is based on a more basic assumption that $f(\mathcal{G}_i), f(\mathcal{H}_i)$ follow Gaussian distributions, which presumes that random reindexing only introduces Gaussian noise to the result.

There is no mean difference between the output embeddings of the two graphs if $\boldsymbol{\mu} = \mathbf{0}$, which means the GNN intrinsically cannot distinguish them. Thus the distinguishing result can be obtained by conducting an α -level Hotelling's T-square test of $H_0 : \boldsymbol{\mu} = \mathbf{0}$ versus $H_1 : \boldsymbol{\mu} \neq \mathbf{0}$ [Johnson and Wichern, 2007]. Formally, we first calculate the T^2 -statistic for the mean difference $\boldsymbol{\mu}$:

$$T^2 = q(\bar{\mathbf{d}} - \boldsymbol{\mu})^T \mathbf{S}^{-1}(\bar{\mathbf{d}} - \boldsymbol{\mu}), \quad (4)$$

where

$$\bar{\mathbf{d}} = \frac{1}{q} \sum_{i=1}^q \mathbf{d}_i, \mathbf{S} = \frac{1}{q-1} \sum_{i=1}^q (\mathbf{d}_i - \bar{\mathbf{d}})(\mathbf{d}_i - \bar{\mathbf{d}})^T. \quad (5)$$

To test $H_0 : \boldsymbol{\mu} = \mathbf{0}$, we let $\boldsymbol{\mu} = \mathbf{0}$ in Equation (4) to obtain $T_{test}^2 = q\bar{\mathbf{d}}^T \mathbf{S}^{-1}\bar{\mathbf{d}}$. Then, given a specific α , an α -level test of $H_0 : \boldsymbol{\mu} = \mathbf{0}$ versus $H_1 : \boldsymbol{\mu} \neq \mathbf{0}$ for an $\mathcal{N}(\boldsymbol{\mu}, \boldsymbol{\Sigma})$ population accepts H_0 (the

GNN cannot distinguish the pair) if the observed

$$T_{test}^2 = q\bar{\mathbf{d}}^T \mathbf{S}^{-1} \bar{\mathbf{d}} < \frac{(q-1)d}{(q-d)} F_{d,q-d}(\alpha), \quad (6)$$

where $F_{d,q-d}(\alpha)$ is the upper (100α) th percentile of the F -distribution $F_{d,q-d}$ [Fisher, 1950] with d and $q-d$ degrees of freedom. Similarly, we reject H_0 (the GNN can distinguish the pair) if

$$T_{test}^2 = q\bar{\mathbf{d}}^T \mathbf{S}^{-1} \bar{\mathbf{d}} > \frac{(q-1)d}{(q-d)} F_{d,q-d}(\alpha). \quad (7)$$

Reliability check. Although the above test is theoretically sound in assessing the expressiveness of GNNs, in practice, it still faces the impact of computational precision. This impact can occur in several places, including comparing two numbers close to zero, inverting a matrix close to zero, etc., making it still difficult to constantly rely on the test. Therefore, we include an additional step called reliability check, which aims to monitor abnormal results. This part is implemented in an easy way by bridging external difference between two graphs and internal fluctuations within one graph.

Without loss of generality, we replace the second graph \mathcal{H} by a reindexing of \mathcal{G} , i.e., \mathcal{G}^π , where π is a permutation of $[n]$. Thus, we can obtain the internal fluctuations of \mathcal{G} by comparing \mathcal{G} and \mathcal{G}^π , and the external difference between \mathcal{G} and \mathcal{H} by comparing \mathcal{G} and \mathcal{H} . We utilize the same step as Major procedure on \mathcal{G} and \mathcal{G}^π , calculating the T^2 -statistic as follows:

$$T_{reliability}^2 = q\bar{\mathbf{d}}^T \mathbf{S}^{-1} \bar{\mathbf{d}}, \quad (8)$$

where

$$\bar{\mathbf{d}} = \frac{1}{q} \sum_{i=1}^q \mathbf{d}_i, \quad \mathbf{d}_i = f(\mathcal{G}_i) - f(\mathcal{G}_i^\pi), \quad i \in [q], \quad \mathbf{S} = \frac{1}{q-1} \sum_{i=1}^q (\mathbf{d}_i - \bar{\mathbf{d}})(\mathbf{d}_i - \bar{\mathbf{d}})^T. \quad (9)$$

Recalling that \mathcal{G} and \mathcal{G}^π are isomorphic, the GNN should not separate them, i.e., $\boldsymbol{\mu} = \mathbf{0}$. Therefore, the test result is considered reliable only if $T_{reliability}^2 < \frac{(q-1)d}{(q-d)} F_{d,q-d}(\alpha)$.

Combining the two procedures, we obtain the full RPC (shown in Fig 3): For each pair \mathcal{G} and \mathcal{H} , we first calculate $Threshold = \frac{(q-1)d}{(q-d)} F_{d,q-d}(\alpha)$, and then perform the Major procedure on \mathcal{G} and \mathcal{H} and the Reliability check on \mathcal{G} and \mathcal{G}^π . Only if $T_{test}^2 > Threshold$ and $T_{reliability}^2 < Threshold$, we consider that the GNN can distinguish the \mathcal{G} and \mathcal{H} . Empirically, RPC brings much more reliable results than directly comparing $f(\mathcal{G})$ and $f(\mathcal{H})$, which align better with the theory.

We further propose **Reliable Adaptive Pairwise Comparison (RAPC)**, aiming to adaptively adjusting the threshold and providing bound of false positive rate. In practice, we use **RPC** due to the less time consumption and good performance. More details about RAPC can be found in Appendix E.

5 Experiment

In this section, we test the expressiveness of 16 representative models on our BREC dataset.

Model selection. We mainly focus on three types of methods: non-GNN methods, subgraph-based GNNs and k -WL-hierarchy-based GNNs. We implemented 4 types of non-GNN baselines according to Papp and Wattenhofer [2022], which are WL test (3-WL), counting substructures (S_3 and S_4), neighborhood up to radius (N_1 and N_2), and marking (M_1). We implemented these methods by adding additional features during the WL test update or using heterogeneous hashing. Note that these methods usually carry more theoretical meaning than practical meaning, since they require enumerating all 3-node/4-node substructures around nodes (S_3 and S_4), performing exact isomorphism encoding of 1-hop/2-hop ego-nets (N_1 and N_2), or enumerating all 1-node-marked subgraphs for each node (M_1). We additionally included 10 state-of-the-art, more powerful GNNs, focusing mainly on subgraph-based and k -WL-based approaches, including NGNN [Zhang and Li, 2021], DS-GNN/DSS-GNN [Bevilacqua et al., 2021], GNN-AK [Zhao et al., 2022a], SUN [Frasca et al., 2022], PPGN [Maron et al., 2019], DE+NGNN [Li et al., 2020], KP-GNN [Feng et al., 2022], KC-SetGNN [Zhao et al., 2022b] and I²GNN [Huang et al., 2022].

Table 2 shows the main comparison results. N_2 achieves the highest accuracy among all non-GNN baselines, and I²-GNN achieves the highest accuracy among all GNN baselines. We detail each

Table 2: Pair distinguishing accuracies on BREC

Model	Basic Graphs (60)		Regular Graphs (140)		Extension Graphs (100)		CFI Graphs (100)		Total (400)	
	Number	Accuracy	Number	Accuracy	Number	Accuracy	Number	Accuracy	Number	Accuracy
3-WL	60	100%	50	35.7%	100	100%	60	60.0%	270	67.5%
S_3	52	86.7%	48	34.3%	5	5%	0	0%	105	26.2%
S_4	60	100%	99	70.7%	84	84%	0	0%	243	60.8%
N_1	60	100%	99	85%	93	93%	0	0%	252	63%
N_2	60	100%	138	98.6%	100	100%	0	0%	298	74.5%
M_1	60	100%	50	35.7%	100	100%	41	41%	251	62.8%
NGNN	59	98.3%	48	34.3%	59	59%	0	0%	166	41.5%
DS-GNN	58	96.7%	48	34.3%	100	100%	18	18%	224	56%
DSS-GNN	58	96.7%	48	34.3%	100	100%	16	16%	222	55.5%
SUN	60	100%	50	35.7%	100	100%	16	16%	226	56.5%
PPGN	60	100%	50	35.7%	100	100%	26	26%	236	59%
GNN-AK	60	100%	50	35.7%	97	97%	15	15%	222	55.5%
DE+NGNN	60	100%	50	35.7%	100	100%	23	23%	233	58.2%
KP-GNN	60	100%	106	75.7%	98	98%	11	11%	275	68.8%
KC-SetGNN	60	100%	50	35.7%	100	100%	1	1%	211	52.8%
I ² -GNN	60	100%	100	71.4%	100	100%	23	23%	283	70.8%

baseline’s accuracy on different types of graphs, showing that it matches with known theoretical results well. Detailed experiment settings are included in Appendix H.

Non-GNN baselines. 3-WL successfully distinguishes all Basic graphs, Extension graphs, simple regular graphs and 60 CFI graphs as expected. S_3 , S_4 , N_1 , and N_2 perform excellently in small-radius graphs, including Basic graphs, Regular graphs and Extension graphs. However, since the receptive field is restricted, they cannot distinguish large-radius graphs like CFI graphs. The expressiveness of S_3 and S_4 are bounded by N_1 and N_2 , respectively, following the theoretical analysis by Papp and Wattenhofer [2022]. M_1 is realized by a heterogenous message passing, thus will not be affected by large graph diameters in CFI graphs.

Subgraph-based GNNs. For subgraph-based models, they can generally distinguish almost all Basic graphs, simple regular graphs and Extension graphs. An exception is NGNN, which performs poorly in Extension graphs due to its simple node selection policy and not using any node labeling. The other two exceptions are KP-GNN and I²GNN, which perform greatly in Regular graphs. KPGNN can distinguish a large number of strongly regular graphs and 4-vertex condition graphs, leading to stronger-than-3-WL power in some cases. I²GNN also overcomes 3-WL with better cycle-counting power. A critical factor affecting the performance of subgraph GNNs is the subgraph radius. Methods with proper encoding functions theoretically have better performance with subgraph radius increasing. However, in practice, increasing radius may lead to information smoothing since the receptive field is enlarged and some information useless for distinguishing or noise may be included. Thus, we treat it as a hyperparameter and tune it for each model, and report the best results in Table 2. Further details on the radius selection can be found in Appendix F.

Comparing different subgraph GNNs, KP-GNN can discriminate part of the strongly regular graphs by peripheral subgraphs, which brings higher performance. Distance encoding can better discriminate different hops for a certain subgraph radius, leading to higher discriminative ability in a larger subgraph radius, which is utilized in DE+NGNN and I²GNN. DS-GNN, DSS-GNN, GNN-AK and SUN adopt similar aggregation schemes with slightly different operations. Their performance is similar, and SUN performs slightly better than others, which is expected since SUN is a more complex model with higher expressiveness.

k -WL hierarchy-based GNNs. For the k -WL-hierarchy-based models, we select two implementation ideas of the method: high-order simulation and local-WL simulation. The representative work of the former is chosen as PPGN, while the latter is chosen as KCSet-GNN. For PPGN, they can generally follow 3-WL’s performance in all types of graphs except the CFI graphs. With larger diameters, CFI graphs require more WL iterations (layers of GNNs). However, a large number of layers may encounter the problem of over-smoothing, causing a gap between theoretical results and actual performance. Nevertheless, PPGN still outperforms other GNNs in CFI graphs as global k -WL keeps every k -tuple whether connected or not. For KCSet-GNN, we set $k = 3, c = 2$ to simulate local 3-WL following the original setting. Comparing the output results for regular graphs with relatively small diameters, we found that local-WL methods can match the performance of general k -WL. In contrast, for CFI graphs with larger radii, local-WL methods have lower performance due to insufficient receptive field.

6 Future Work

Apart from the expressiveness comparison based on GI, there are some other metrics for GNN expressiveness evaluation, including substructure counting, diameter counting and bio-connectivity checking, etc. However, these tests are often conducted on datasets not designed for expressiveness comparison [Huang et al., 2022], which may lead to biased results caused by spurious correlations. That is, some methods may not be able to count a specific substructure but can capture another property that happens to associate with the substructure count, leading to false high performance. This problem can be alleviated in BREC because of the high difficulty. We reveal the data generation process of BREC in Appendix I, hoping that researchers can utilize them in more tasks.

7 Conclusion

In this paper, we propose a new dataset, BREC, for GNN expressiveness comparison. BREC addresses the limitations of previous datasets, including difficulty, granularity, and scale, by incorporating 400 pairs of diverse graphs in four categories. A new evaluation method is proposed for principled expressiveness evaluation. Finally, a thorough comparison of 16 baselines on BREC is conducted.

References

- David K Duvenaud, Dougal Maclaurin, Jorge Iparraguirre, Rafael Bombarell, Timothy Hirzel, Alán Aspuru-Guzik, and Ryan P Adams. Convolutional networks on graphs for learning molecular fingerprints. *Advances in neural information processing systems*, 28, 2015.
- Albert-László Barabási, Natali Gulbahce, and Joseph Loscalzo. Network medicine: a network-based approach to human disease. *Nature reviews genetics*, 12(1):56–68, 2011.
- Wenqi Fan, Yao Ma, Qing Li, Yuan He, Eric Zhao, Jiliang Tang, and Dawei Yin. Graph neural networks for social recommendation. In *The world wide web conference*, pages 417–426, 2019.
- Hongwei Wang, Fuzheng Zhang, Jialin Wang, Miao Zhao, Wenjie Li, Xing Xie, and Minyi Guo. Ripplenet: Propagating user preferences on the knowledge graph for recommender systems. In *Proceedings of the 27th ACM international conference on information and knowledge management*, pages 417–426, 2018a.
- Rianne van den Berg, Thomas N Kipf, and Max Welling. Graph convolutional matrix completion. *arXiv preprint arXiv:1706.02263*, 2017.
- Jie Zhou, Ganqu Cui, Shengding Hu, Zhengyan Zhang, Cheng Yang, Zhiyuan Liu, Lifeng Wang, Changcheng Li, and Maosong Sun. Graph neural networks: A review of methods and applications. *AI open*, 1:57–81, 2020.
- Keyulu Xu, Weihua Hu, Jure Leskovec, and Stefanie Jegelka. How powerful are graph neural networks? *arXiv preprint arXiv:1810.00826*, 2018.
- Muhammet Balciilar, Pierre Héroux, Benoit Gauzere, Pascal Vasseur, Sébastien Adam, and Paul Honeine. Breaking the limits of message passing graph neural networks. In *International Conference on Machine Learning*, pages 599–608. PMLR, 2021.
- Beatrice Bevilacqua, Fabrizio Frasca, Derek Lim, Balasubramaniam Srinivasan, Chen Cai, Gopinath Balamurugan, Michael M Bronstein, and Haggai Maron. Equivariant subgraph aggregation networks. *arXiv preprint arXiv:2110.02910*, 2021.
- Leonardo Cotta, Christopher Morris, and Bruno Ribeiro. Reconstruction for powerful graph representations. *Advances in Neural Information Processing Systems*, 34:1713–1726, 2021.
- Christopher Morris, Martin Ritzert, Matthias Fey, William L Hamilton, Jan Eric Lenssen, Gaurav Rattan, and Martin Grohe. Weisfeiler and leman go neural: Higher-order graph neural networks. In *Proceedings of the AAAI conference on artificial intelligence*, volume 33, pages 4602–4609, 2019.

- Jiaxuan You, Jonathan M Gomes-Selman, Rex Ying, and Jure Leskovec. Identity-aware graph neural networks. In *Proceedings of the AAAI conference on artificial intelligence*, volume 35, pages 10737–10745, 2021.
- Muhan Zhang and Pan Li. Nested graph neural networks. *Advances in Neural Information Processing Systems*, 34:15734–15747, 2021.
- Haggai Maron, Heli Ben-Hamu, Nadav Shamir, and Yaron Lipman. Invariant and equivariant graph networks. *arXiv preprint arXiv:1812.09902*, 2018.
- Fabrizio Frasca, Beatrice Bevilacqua, Michael Bronstein, and Haggai Maron. Understanding and extending subgraph gnns by rethinking their symmetries. *Advances in Neural Information Processing Systems*, 35:31376–31390, 2022.
- Bohang Zhang, Guhao Feng, Yiheng Du, Di He, and Liwei Wang. A complete expressiveness hierarchy for subgraph gnns via subgraph weisfeiler-lehman tests. *arXiv preprint arXiv:2302.07090*, 2023a.
- Pál András Papp and Roger Wattenhofer. A theoretical comparison of graph neural network extensions. In *International Conference on Machine Learning*, pages 17323–17345. PMLR, 2022.
- Jiarui Feng, Yixin Chen, Fuhai Li, Anindya Sarkar, and Muhan Zhang. How powerful are k-hop message passing graph neural networks. In Alice H. Oh, Alekh Agarwal, Danielle Belgrave, and Kyunghyun Cho, editors, *Advances in Neural Information Processing Systems*, 2022. URL <https://openreview.net/forum?id=nN3aVRQsxGd>.
- Yinan Huang, Xingang Peng, Jianzhu Ma, and Muhan Zhang. Boosting the cycle counting power of graph neural networks with i^2 -gnns. *arXiv preprint arXiv:2210.13978*, 2022.
- Bohang Zhang, Shengjie Luo, Liwei Wang, and Di He. Rethinking the expressive power of gnns via graph biconnectivity. In *The Eleventh International Conference on Learning Representations*, 2023b.
- Ralph Abboud, Ismail Ilkan Ceylan, Martin Grohe, and Thomas Lukasiewicz. The surprising power of graph neural networks with random node initialization. *arXiv preprint arXiv:2010.01179*, 2020.
- Ryan Murphy, Balasubramaniam Srinivasan, Vinayak Rao, and Bruno Ribeiro. Relational pooling for graph representations. In *International Conference on Machine Learning*, pages 4663–4673. PMLR, 2019.
- Richard A. Johnson and Dean W. Wichern. *Applied multivariate statistical analysis*. Pearson Prentice Hall, Upper Saddle River, N.J, 6th ed edition, 2007. ISBN 978-0-13-187715-3. OCLC: ocm70867129.
- Zhengdao Chen, Soledad Villar, Lei Chen, and Joan Bruna. On the equivalence between graph isomorphism testing and function approximation with gnns. *Advances in neural information processing systems*, 32, 2019.
- Floris Geerts and Juan L Reutter. Expressiveness and approximation properties of graph neural networks. *arXiv preprint arXiv:2204.04661*, 2022.
- Boris Weisfeiler and Andrei Leman. The reduction of a graph to canonical form and the algebra which appears therein. *nti, Series*, 2(9):12–16, 1968.
- J.-Y. Cai, M. Furer, and N. Immerman. An optimal lower bound on the number of variables for graph identification. In *30th Annual Symposium on Foundations of Computer Science*, pages 612–617, 1989. doi: 10.1109/SFCS.1989.63543.
- Pan Li, Yanbang Wang, Hongwei Wang, and Jure Leskovec. Distance encoding: Design provably more powerful neural networks for graph representation learning. *Advances in Neural Information Processing Systems*, 33:4465–4478, 2020.
- AE Brouwer, F Ihringer, and WM Kantor. Strongly regular graphs satisfying the 4-vertex condition. *arXiv preprint arXiv:2107.00076*, 2021.

- Andries E Brouwer, Willem H Haemers, Andries E Brouwer, and Willem H Haemers. Strongly regular graphs. *Spectra of graphs*, pages 115–149, 2012a.
- Andries E Brouwer, Willem H Haemers, Andries E Brouwer, and Willem H Haemers. *Distance-regular graphs*. Springer, 2012b.
- Gregory Koch, Richard Zemel, Ruslan Salakhutdinov, et al. Siamese neural networks for one-shot image recognition. In *ICML deep learning workshop*, volume 2. Lille, 2015.
- Raia Hadsell, Sumit Chopra, and Yann LeCun. Dimensionality reduction by learning an invariant mapping. In *2006 IEEE Computer Society Conference on Computer Vision and Pattern Recognition (CVPR’06)*, volume 2, pages 1735–1742. IEEE, 2006.
- Hao Wang, Yitong Wang, Zheng Zhou, Xing Ji, Dihong Gong, Jingchao Zhou, Zhifeng Li, and Wei Liu. Cosface: Large margin cosine loss for deep face recognition. In *Proceedings of the IEEE conference on computer vision and pattern recognition*, pages 5265–5274, 2018b.
- Ronald Aylmer Fisher. Contributions to mathematical statistics. 1950.
- Lingxiao Zhao, Wei Jin, Leman Akoglu, and Neil Shah. From stars to subgraphs: Uplifting any GNN with local structure awareness. In *International Conference on Learning Representations*, 2022a. URL https://openreview.net/forum?id=Mspk_WYKoEH.
- Haggai Maron, Heli Ben-Hamu, Hadar Serviansky, and Yaron Lipman. Provably powerful graph networks. *Advances in neural information processing systems*, 32, 2019.
- Lingxiao Zhao, Neil Shah, and Leman Akoglu. A practical, progressively-expressive gnn. *Advances in Neural Information Processing Systems*, 35:34106–34120, 2022b.
- László Babai and Ludik Kucera. Canonical labelling of graphs in linear average time. In *20th Annual Symposium on Foundations of Computer Science (sfcs 1979)*, pages 39–46. IEEE, 1979.
- Ryoma Sato. A survey on the expressive power of graph neural networks. *arXiv preprint arXiv:2003.04078*, 2020.
- Ningyuan Teresa Huang and Soledad Villar. A short tutorial on the weisfeiler-lehman test and its variants. In *ICASSP 2021-2021 IEEE International Conference on Acoustics, Speech and Signal Processing (ICASSP)*, pages 8533–8537. IEEE, 2021.

A Details on Regular Graphs

In this section, we introduce the relationship between four types of regular graphs. The inclusion relations of them are shown in Figure 4, but their difficulty relations and inclusion relations are not consistent.

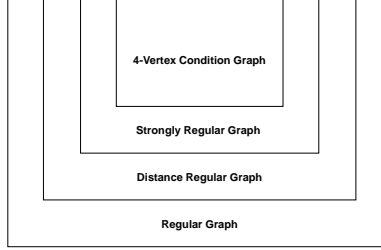


Figure 4: Regular graphs relationship

A graph is a regular graph if all the vertices have the same degree. A regular graph with v vertices and degree k is strongly regular if there are integers λ and μ such that every two adjacent vertices have λ common neighbors and every two non-adjacent vertices have μ common neighbors. Thus it can be denoted as $\text{srg}(v, k, \lambda, \mu)$ with four parameters.

Regular graphs and strongly regular graphs are widely used for expressiveness analysis. The difficulty of strongly regular graphs is greatly increased compared to general regular graphs since they include additional requirements. The simplest strongly regular graphs with the same parameters ($\text{srg}(16, 6, 2, 2)$) are the Shrikhande graph and 4×4 -Rook's graph, as shown in Figure 2(c)).

4-vertex condition graphs and distance regular graphs increase the difficulty but with opposite development directions. 4-vertex condition graph is a strongly regular graph with an additional property. It further requires the number of edges between 2 vertices' common neighbors to be determined by whether the two vertices are connected. Distance regular graphs, however, are implemented by expanding the definition of strongly regular graphs. A distance regular graph is a regular graph such that for any two vertices v and w , the number of vertices at a distance j from v and at a distance k from w depends only upon j, k and the distance between v and w . A distance regular graph with radius = 2 is a strongly regular graph.

The 4-vertex condition graph has yet to be considered in previous studies. The examples of distance regular graphs are also relatively rare and difficult to analyze by example. We added them to BREC to motivate relevant research further.

B Node Features

In this section, we introduce node features and edge features in graphs.

We first give the definition of graphs with the adjacent matrix. Supposing a graph with node feature represented by d_n -dim vector and edge feature represented by d_e -dim vector, it is denoted $\mathcal{G} = (\mathbf{V}(\mathcal{G}), \mathbf{E}(\mathcal{G}))$, with $\mathbf{V}(\mathcal{G}) \in \mathbb{R}^{n \times d_n}$ and $\mathbf{E}(\mathcal{G}) \in \mathbb{R}^{n \times n \times (d_e + 1)}$, where n is the number of nodes in the graph. The adjacent matrix of the graph is $\mathbf{A}(\mathcal{G}) \in \mathbb{R}^{n \times n} = \mathbf{E}(\mathcal{G})_{::, (d_e + 1)}$, where $\mathbf{A}(\mathcal{G})_{i,j} = 1$ if $(i, j) \in \mathbb{E}(\mathcal{G})$, otherwise $\mathbf{A}(\mathcal{G})_{i,j} = 0$. Feature of node i is $\mathbf{V}(\mathcal{G})_{i,:}$, and feature of edge (i, j) is $\mathbf{E}(\mathcal{G})_{i,j, 1:d_e}$. The permutation(or reindexing) of \mathcal{G} is denoted as $\mathcal{G}^\pi = (\mathbf{V}(\mathcal{G}), \mathbf{E}(\mathcal{G}))$ with permutation $\pi : [n] \rightarrow [n]$, s.t. $\mathbf{V}(\mathcal{G})_{i,:} = \mathbf{V}(\mathcal{G})_{\pi(i),:}$, $\mathbf{E}(\mathcal{G})_{i,j,:} = \mathbf{E}(\mathcal{G})_{\pi(i), \pi(j),:}$.

Then we discuss the usage of features. It is obvious including node features in initialization and edge features in message passing will benefit the performance of GNNs with suitable hyperparameters and training. However, can features represent graph structures or can they bring extra expressiveness? Let us first separate features into two types. One type is to fully use original features, such as distance to other nodes or spectral embeddings. Another type is to add additional features, such as manually selected node identifiers. The former type can help GNN solve GI, but that is caused by decreased difficulty instead of increased expressiveness. Suppose we want to recognize the 6-cycle in a graph. We can manually find a 6-cycle, and mark each node in the 6-cycle with a distinctive feature. Then

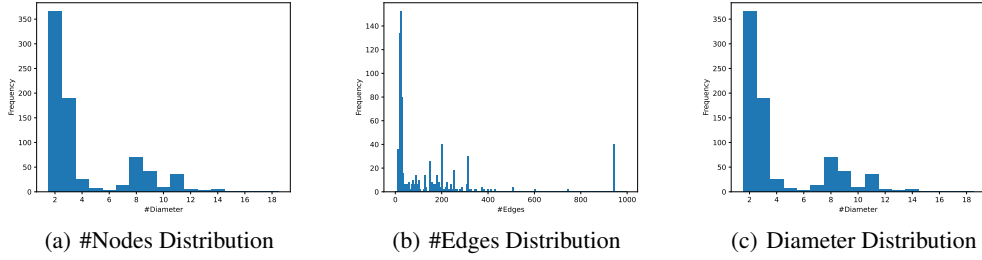


Figure 5: BREC Statistics

the GNN can recognize by aggregating the six distinctive features. However, this does not bring extra ability with the GNN, so as its other abilities for more tasks. The latter type actually requires dedicated design to utilize these features. For example, only with global aggregation can the GNN utilize distance between nodes, while a simple MPNN can not use it. Overall, we can answer the question as follows. Features can bring expressiveness, but this should be done on models, instead of datasets. For BREC, a dataset for testing expressiveness, we do not include other meaningful features. We only use the same vector for all node features and edge features and follow specific model settings to add graph original features, like the distance between nodes.

C WL Algorithm

In this section, we briefly introduce the WL algorithm and two high-order variants.

1-WL is the original WL algorithm. It is a graph isomorphism algorithm, which can be used to generate a unique label for each graph. Each node keeps a state (or color) that gets refined in each iteration by aggregating information from their neighbors' states. The final graph representation is a multiset of node states when converging.

In order to step over those examples, some researchers managed to extend each node in the 1-WL test to a larger unit, leading to the k -WL test [Babai and Kucera, 1979, Morris et al., 2019]. The k -dimensional Weisfeiler Lehman test extends the test to coloring k -tuples of nodes.

Cai et al. [1989] also proposed a WL test algorithm extending to k -tuples. However, the processing varied from the k -WL test in detail. It is commonly named the k -FWL(k -folklore-WL) test. The major difference between k -WL and k -FWL is the definition of neighbor and order of aggregating from tuples and multisets.

There are three interesting results:

- 1 1-WL = 2-WL
- 2 k -WL $>$ $(k - 1)$ -WL, $(k > 2)$
- 3 $(k - 1)$ -FWL = k -WL

More details can be found in Sato [2020], Huang and Villar [2021].

D BREC Statistics

Here we give some statistics of BREC dataset, shown in Figure 5.

E RAPC: a Reliable and Adaptive Evaluation Method

In this section, we propose RAPC with an additional stage called adaptive confidence interval based on RPC. Though RPC performs excellently in experiments with a general theoretical guarantee in reliability, with manually setting α . we still want to make the procedure more automated. In addition, we found that the inner fluctuations of each pair, i.e. $T_{reliability}^2$, vary from pairs. This means some graph outputs are more stable than others, and the threshold of them can be larger than others. However, it is impossible to manually set the confidence interval (α) for all pairs, thus we

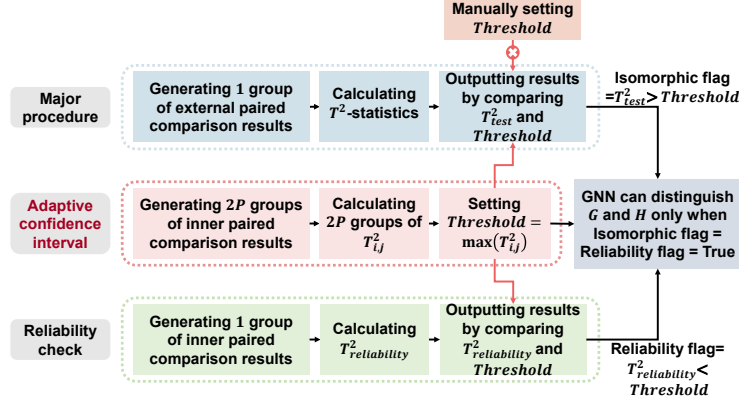


Figure 6: RAPC pipeline.

propose an adaptive confidence interval method to solve this problem. The key idea is to set the threshold according to minimum internal fluctuations.

Given a pair of non-isomorphic graphs \mathcal{G} and \mathcal{H} to be tested. For simplicity, we rename \mathcal{G} as \mathcal{G}_1 , \mathcal{H} as \mathcal{G}_2 . For each graph (\mathcal{G}_1 and \mathcal{G}_2), we generate p groups of graphs, with each group containing $2q$ graphs, represented by:

$$\mathcal{G}_{i,j,k}, i \in [2], j \in [p], k \in [2q]. \quad (10)$$

Similarly, we can calculate T^2 -statistics for each group ($2p$ groups in total):

$$T_{i,j}^2 = q \bar{\mathbf{d}}_{i,j}^T \mathbf{S}_{i,j} \bar{\mathbf{d}}_{i,j}, i \in [2], j \in [p]. \quad (11)$$

where

$$\begin{aligned} \bar{\mathbf{d}}_{i,j} &= \frac{1}{q} \sum_{k=1}^q \mathbf{d}_{i,j,k}, \mathbf{d}_{i,j,k} = f(\mathcal{G}_{i,j,k}) - f(\mathcal{G}_{i,j,k+q}), i \in [2], j \in [p], k \in [q], \\ \mathbf{S}_{i,j} &= \frac{1}{q-1} \sum_{j=1}^q (\mathbf{d}_{i,j,k} - \bar{\mathbf{d}}_{i,j})(\mathbf{d}_{i,j,k} - \bar{\mathbf{d}}_{i,j})^T. \end{aligned} \quad (12)$$

Similar to major procedure, we can conduct an α -level test of $H_0 : \delta = \mathbf{0}$ versus $H_1 : \delta \neq \mathbf{0}$, it should always accept H_0 (the GNN cannot distinguish them) since the $2q$ graphs in each group are essentially the same. And T^2 -statistics should satisfy the:

$$T_{i,j}^2 = q \bar{\mathbf{d}}_{i,j}^T \mathbf{S}_{i,j} \bar{\mathbf{d}}_{i,j} < \frac{(q-1)n}{(q-n)} F_{n,q-n}(\alpha). \quad (13)$$

If the GNN can distinguish the pair, T_{test}^2 in major procedure and $T_{i,j}^2$ in adaptive confidence interval should satisfy the:

$$T_{test}^2 > \frac{(q-1)n}{(q-n)} F_{n,q-n}(\alpha) > T_{i,j}^2, \forall i \in [2], j \in [p]. \quad (14)$$

Thus we set the adaptive confidence interval as $Threshold = \max_{i \in \{1,2\}, p \in \{1, \dots, P\}} \{T_{i,p}^2\}$. Then we conduct Major Procedure and Reliability Check based on $Threshold$ similar to RPC. The pipeline is shown in Fig 6.

We analyze the current evaluation method by considering the probability of false positives and false negatives. In general, it is difficult to control the probability of both simultaneously at extremely low levels, and a trade-off is often required. Noting that false positives compromise the reliability of methods, we give priority to giving strict bounds to this class of errors, while false negatives give an intuitive explanation.

Regarding false positives, we give the following theorem.

Theorem E.1. The false positive rate with adaptive confidence interval is $\frac{1}{2^{2P}}$.

Table 3: A general theoretical expressiveness upper bound of subgraph with radius k

Radius	1	2	3	4	5	6	7	8	9	10
#Accurate on BREC	252	298	300	327	326	385	398	398	399	400

Proof. We first define false positives more formally. False positives mean the GNN f cannot distinguish \mathcal{G} and \mathcal{H} , but we reject H_0 and accept H_1 . f cannot distinguish \mathcal{G} and \mathcal{H} means $f(\mathcal{G}) = f(\mathcal{H}) = f(\mathcal{G}^\pi) \sim \mathcal{N}(\boldsymbol{\mu}_{\mathcal{G}}, \boldsymbol{\Sigma}_{\mathcal{G}})$. Since \mathbf{d}_i in major procedure and $\mathbf{d}_{i,j,k}$ in adaptive confidence interval are derived from paired comparison by same function outputs, i.e., from $f(\mathcal{G})$ and $f(\mathcal{H})$, and from $f(\mathcal{G})$ and $f(\mathcal{G}^\pi)$, respectively. \mathbf{d}_i and $\mathbf{d}_{i,j,k}$ should follow the same distribution, leading that T_{test}^2 and $T_{i,j}^2$ are independently random variables following the same distribution. Thus $P(T_{test}^2 > T_{i,j}^2) = \frac{1}{2}$. Then we can calculate the probability of false positives as

$$P(\text{Rejecting } H_0) = P(T_{test}^2 > \text{Threshold} = \text{Max}_{i \in [2], j \in [p]} \{T_{i,j}^2\}) = \frac{1}{2^{2p}}. \quad (15)$$

Thus we proof theorem E.1. \square

Regarding false negatives, we propose the following explanation. A small threshold can decrease the false negative rate. Thus without compromising the rest of the theoretical analysis, we give the minimum value of the threshold. Equation 13 introduces a minimum threshold restriction. We obtain the threshold strictly based on it by taking the maximum value, which is the theoretical minimum threshold that minimizes the false negative rate.

F Subgraph GNNs

In this section, we discuss settings for subgraph GNN models. The most important setting is the subgraph radius. As discussed before, a larger radius can capture more structural information, increasing the model’s expressiveness. However, it will include more invalid information, making it harder to reach the theoretical upper bound. Thus we need to find a balance between the two.

To achieve this, we first explore the maximum structural information that can be obtained under a given radius. Following Papp and Wattenhofer [2022], we implement N_k method, which embeds the isomorphic type of k -hop subgraph when initializing. This method is only available in the theoretical analysis as one can not solve the GI problem by manually giving graph isomorphic type. We mainly use it as a general expressiveness upper bound of subgraph GNNs. The performance of N_k on BREC is shown in Table 3. Actually, N_3 already successfully distinguishes all graphs except for CFI graphs. $k = 6$ is an important threshold as N_k outperforms 3-WL (expressiveness upper bound for most subgraph GNNs [Frasca et al., 2022, Zhang et al., 2023a]) in all types of graphs. An interesting discovery is that increasing the radius does not always lead to expressiveness increasing as expected. This is caused by the fact that we only encode the exact k -hop subgraph instead of 1 to k -hop subgraphs. This phenomenon is similar to subgraph GNNs, revealing the advantages of using distance encoding.

We then test the subgraph GNNs’ radii by increasing them until reaching the best performance, which is expected to be a perfect balance. For most methods, radius= 6 is the best selection, which is consistent with the theory. The three exceptions are NGNN, NGNN+DE, and KPGNN. NGNN directly uses an inner GNN to calculate subgraph representation, whose expressiveness is restricted by the inner GNN. As the subgraph radius increases, though the subgraph contains information, the simple inner GNN can hardly give correct representation. That’s why radius= 1 is the best setting for NGNN. NGNN+DE adds distance encoding to NGNN, making the subgraph with a large radius can always clearly extract a subgraph with a small radius. Therefore, a large radius= 8 is available. KPGNN utilizes a similar setting by incorporating distance to subgraph representation, and radius= 8 is also the best setting. KPGNN can also use graph diffusion to replace the shortest path distance. Though graph diffusion outperforms some graphs, the shortest path distance is generally a better solution. Previous findings reveal the advantages of using distance, which we hope can be more widely used in further research.

Table 4: The performance of 3-WL with different iteration times

Iterations	1	2	3	4	5
#Accurate on BREC	193	209	217	264	270

Table 5: Model Hyperparameters

Model	Radius	Layers	Inner dim	Threshold	Learning rate	Weight decay	Batch size	Epoch	Early stop threshold
NGNN	1	6	16	20.0	$1e-4$	$1e-5$	32	20	0.2
DS-GNN	6	10	32	10.0	$1e-4$	$1e-5$	32	10	0.01
DSS-GNN	6	9	32	10.0	$1e-4$	$1e-4$	32	10	0.3
SUN	6	9	32	10.0	$1e-4$	$1e-4$	32	10	0.3
PPGN	/	5	32	10.0	$1e-4$	$1e-4$	32	20	0.2
GNN-AK	6	4	32	10.0	$1e-4$	$1e-4$	32	10	0.1
DE+NGNN	8	6	128	20.0	$1e-4$	$1e-5$	32	20	0.2
KP-GNN	8	8	32	20.0	$1e-4$	$1e-4$	32	20	0.3
KC-SetGNN	/	4	64	10.0	$1e-4$	$1e-4$	16	15	0.3
l^2 GNN	8	5	32	10.0	$1e-5$	$1e-4$	16	20	0.2

G k -WL Hierarchy GNNs

In this section, we discuss settings for k -WL hierarchy GNN models. k -WL algorithm requires a converged tuple embedding distribution for GI. However, k -WL hierarchy GNNs do not have the definition of converging. It will output the final embeddings after a specific number of layers, i.e., the iteration times of k -WL. Thus we need to give a suitable number of layers where the k -WL converged after the number of iteration times. In theory, increasing the number of layers always leads to a non-decreasing expressiveness, since the converged distribution will not change furthermore. However, more layers may cause over-smoothing, leading to worse performance in practice.

To keep a balance, we utilize similar methods for subgraph GNNs. We first analyze the iteration times of 3-WL, shown in Table 4. One can see 6 iteration times are enough for all types of graphs. Then we increase the layers of k -WL GNNs until reaching the best performance. We finally set 5 layers for PPGN and 4 layers for KCSet-GNN.

H Experiment Settings

RPC settings. For non-GNN methods, since the output results are uniquely determined, this part of the experiment does not require using RPC. Noting that most non-GNN baselines require running graph isomorphism testing software on subgraphs, they mainly serve as some theoretical references. For GNNs, we utilize RPC with $q = 32, d = 16$ to evaluate performance. With confidence level $\alpha = 0.95$ (a typical setting in statistics), the threshold should be set to $\frac{(q-1)d}{(q-d)} F_{d,q-d}(\alpha) = 31F_{16,16}(0.95) = 72.34$. However, in practice, we find that the threshold can be looser. With *Threshold* = 10 or 20, models can pass Reliability check for all graphs. We repeat all the evaluation methods for 10 times with seeds in $\{100, 200, \dots, 1000\}$, and consider the final results reliable only if the model passes Reliability check for all graphs with any seed. The reported results are selected as the best results, instead of average, since we are exploring the upper bound expressiveness.

Training settings. We follow Siamese network design and utilize cosine similarity loss. Another widely used loss function is contrastive loss [Hadsell et al., 2006], which directly calculates the difference between two outputs. The advantage of cosine similarity loss is measuring output difference under the same scale by normalization, instead of unlimitedly enlarging model outputs so that a minor precision error can be amplified and treated as a differentiated result of the model. We use Adam optimizer with learning rate searched in $\{1e-3, 1e-4, 1e-5\}$, weight decay searched in $\{1e-3, 1e-4, 1e-5\}$, and batchsize in $\{16, 32, 64\}$. We adopt an early stop strategy when the loss decreases to a small value. The maximum epoch is set to around 20 because the model typically distinguishes a pair quickly.

Model hyperparameters. The most effective hyperparameters related to expressiveness, i.e., subgraph radius for subgraph GNNs and number of layers for k -WL hierarchy GNNs, are determined with theoretical analysis, referring to Appendix F and G. Other hyperparameters also implicitly influence expressiveness. We mainly follow the same settings in previous expressiveness datasets.

Two exceptions are inner embedding dim and batch norm. Inner embedding dim represents model capacity. For previous small and simple expressiveness datasets, a small embedding dim is enough. However, the appropriate embedding dim on BREC is unknown, thus we search in $\{32, 64, 128\}$. Another setting is the batch norm. Though it was not used in all models, we utilize it for all models. It can control outputs in a suitable range, which is beneficial for distinguishing.

The detailed settings for each method are shown in Table 5.

I Graph Generation

In this section, we discuss how the graphs in BREC are generated.

Basic graphs compose 60 pairs of graphs with 10 nodes. We run 1-WL on all the 11.7 million graphs with 10 nodes, producing 1-WL hash values for each graph. Then we found there are 83074 graphs whose hash values happen to be equal with others. Finally, We randomly selected 60 pairs of graphs.

Regular graphs compose 140 pairs of different kinds of regular graphs. For 50 simple regular graphs, we search regular graphs with 6 - 10 nodes. Then we randomly select 50 pairs of regular graphs with the same parameters. For 50 strongly regular graphs, we set the number of nodes ranging from 16 to 35 (16-node is the most miniature range for pair-wise SRG with the same parameters), refer to <http://www.maths.gla.ac.uk/es/srgraphs.php> and <http://users.cecs.anu.edu.au/bdm/data/graphs.html> for graphs. For 20 4-vertex condition graphs, we search in <http://math.ihringer.org/srgs.php> and select the simplest 20 pairs of 4-vertex condition graphs with the same parameters. For 20 distance regular graphs, we search in <https://www.distanceregular.org/> and select the simplest 20 pairs of distance regular graphs with the same parameters.

Extension graphs compose 100 pairs of graphs based on comparing results between GNN extensions. We run S_3 , S_4 and N_1 on all the 1-WL-indistinguishable graphs with 10 nodes, obtaining 4612 S_3 -indistinguishable graphs, 1132 N_1 -indistinguishable graphs, and 136 S_4 -indistinguishable graphs. We randomly select 60 pairs of S_3 -indistinguishable graphs, 20 pairs of N_1 -indistinguishable graphs, and 10 pairs of S_4 -indistinguishable graphs. We keep that no graphs repeatedly appear. We also add 10 pairs of graphs with a virtual node strategy, including 5 pairs of graphs by adding a virtual node to a 10-node regular graph, and 5 pair of graphs based on C_{2l} and $C_{l,l}$ referring to Papp and Wattenhofer [2022].

CFI graphs compose 100 pairs of graphs based on CFI methods [Cai et al., 1989]. We generate all CFI graphs with backbone ranging from 3 to 7-node graphs. We randomly select 60 pairs of 1-WL-indistinguishable graphs, 20 pairs of 3-WL-indistinguishable graphs, and 20 pairs of 4-WL-indistinguishable graphs.